Current Biology, Vol. 12, 508–513, March 19, 2002, ©2002 Elsevier Science Ltd. All rights reserved. PII S0960-9822(02)00719-4

Condensin Architecture and Interaction with DNA: Regulatory Non-SMC Subunits Bind to the Head of SMC Heterodimer

Shige H. Yoshimura,[1] Kohji Hizume,[1] Akiko Murakami,[2] Takashi Sutani,[1,4] Kunio Takeyasu,[1] and Mitsuhiro Yanagida[1,2,3]
[1]CREST Research Project
Department of Responses to
Environmental Signals and Stresses and
Department of Gene Mechanisms
Graduate School of Biostudies
[2]Department of Biophysics
Graduate School of Science
Kyoto University
Kitashirakawa-Oiwakecho
Sakyo-ku, Kyoto, 606-8502
Japan

Summary

Condensin and cohesin are two protein complexes that act as the central mediators of chromosome condensation and sister chromatid cohesion, respectively. The basic underlying mechanism of action of these complexes remained enigmatic. Direct visualization of condensin and cohesin was expected to provide hints to their mechanisms. They are composed of heterodimers of distinct structural maintenance of chromosome (SMC) proteins and other non-SMC subunits. Here, we report the first observation of the architecture of condensin and its interaction with DNA by atomic force microscopy (AFM). The purified condensin SMC heterodimer shows a head-tail structure with a single head composed of globular domains and a tail with the coiled-coil region. Unexpectedly, the condensin non-SMC trimers associate with the head of SMC heterodimers, producing a larger head with the tail. The heteropentamer is bound to DNA in a distributive fashion, whereas condensin SMC heterodimers interact with DNA as aggregates within a large DNA-protein assembly. Thus, non-SMC trimers may regulate the ATPase activity of condensin by directly interacting with the globular domains of SMC heterodimer and alter the mode of DNA interaction. A model for the action of heteropentamer is presented.

Results and Discussion

Expression, Purification, and Observation of SMC Heterodimer of Condensin Complex

The SMC family of proteins plays a fundamental role in chromosome structure and dynamics [1–3]. They have two globular domains, each of which contains an ATP binding motif, at both termini and a middle long coiled-coil region with a central hinge [4]. Bacterial SMC forms a homodimer [5, 6], and the coiled-coil rod has a flexible central hinge, allowing a "scissoring" action. Eukaryotic SMC may use a similar organizational principle, but its architecture has not been reported. In fission yeast, mutations in SMC proteins (Cut3 and Cut14) were found to block chromosome condensation and sister chromatid separation in mitosis [7]. The purified Cut3-Cut14 heterodimer showed renaturation activity of single-stranded DNAs but no ATPase activity [8]. The SMC proteins have been identified as components of condensin and cohesin complexes in a variety of eukaryotes [9–15]. Condensin and cohesin complex contain three and two non-SMC subunits, respectively [12–16].

To purify the heterodimer, Cut3 and Cut14 were simultaneously expressed in *Schizosaccharomyces pombe* cells under the inducible promoter *nmt1* [8]. The C terminus of Cut14 was tagged with hemagglutinin antigen (HA) and hexa-histidine (H6) for affinity purification (Experimental Procedures). The tagged molecules used were all functional, as they were able to replace the wild-type genes (data not shown). The cell extract containing Cut3-Cut14 HAH6 was loaded onto a Ni-affinity chromatography column and eluted by imidazole, followed by size fractionation. Purity of the isolated Cut3 and Cut14 complex was high, judging from staining patterns by Coomassie brilliant blue (CBB, Figure 1A). The ATPase domain is fully retained in a partially cleaved Cut3 [8].

The observation of the purified heterodimer by AFM revealed abundant head-tail particles (Figure 1B). The head-tail structure can be classified into two major types: long tail (~45 nm) in 70% and short tail (~25 nm) in the remaining population (Figure 1C). The long tail could often be resolved into two, suggesting that it consisted of folded coiled-coil regions. However, the open V-shaped structure frequently seen for prokaryotic SMC homodimers [5] was never observed. The 45 nm tail occasionally kinked showed a protrusion on the tip, possibly representing the hinge (Figure 1B, open triangle).

The average values of the tail length and the head diameter (~28 nm) were obtained (Figure 1D). The total length of the coiled-coil regions predicted from the amino acid sequences of Cut3 and Cut14 is ~90 nm (~600 aa), approximately twice the ~45 nm tail length. One model (Figure 1E) thus is that the heterodimer is folded back at the central hinge such that the single head contains four globular domains. The real diameter of images is known to be exaggerated by the "tip effect" of an AFM probe: a calculation subtracting the effect [17] suggests that the head corresponds to a molecular mass of ~110 kDa, similar to the total molecular weight of the four globular domains of the Cut3/Cut14. For the ~25 nm short tail particle, further folding of the coiled-coil region may take place, possibly due to the interaction between the hinge and the head. For comparison, the SMC heterodimer of cohesin complex (Psm1-Psm3) was overproduced and purified. The isolated cohesin SMC heterodimer Psm1-Psm3 had also a head-tail appearance (see the Supplementary Material available with this article online). As Rad21/Scc1 was highly proteolytic

[3]Correspondence: yanagida@kozo.biophys.kyoto-u.ac.jp
[4]Present address: Department of Molecular and Cellular Biology, Howard Hughes Medical Institute, Harvard University, 7 Divinity Avenue, Cambridge, Massachusetts 02138.

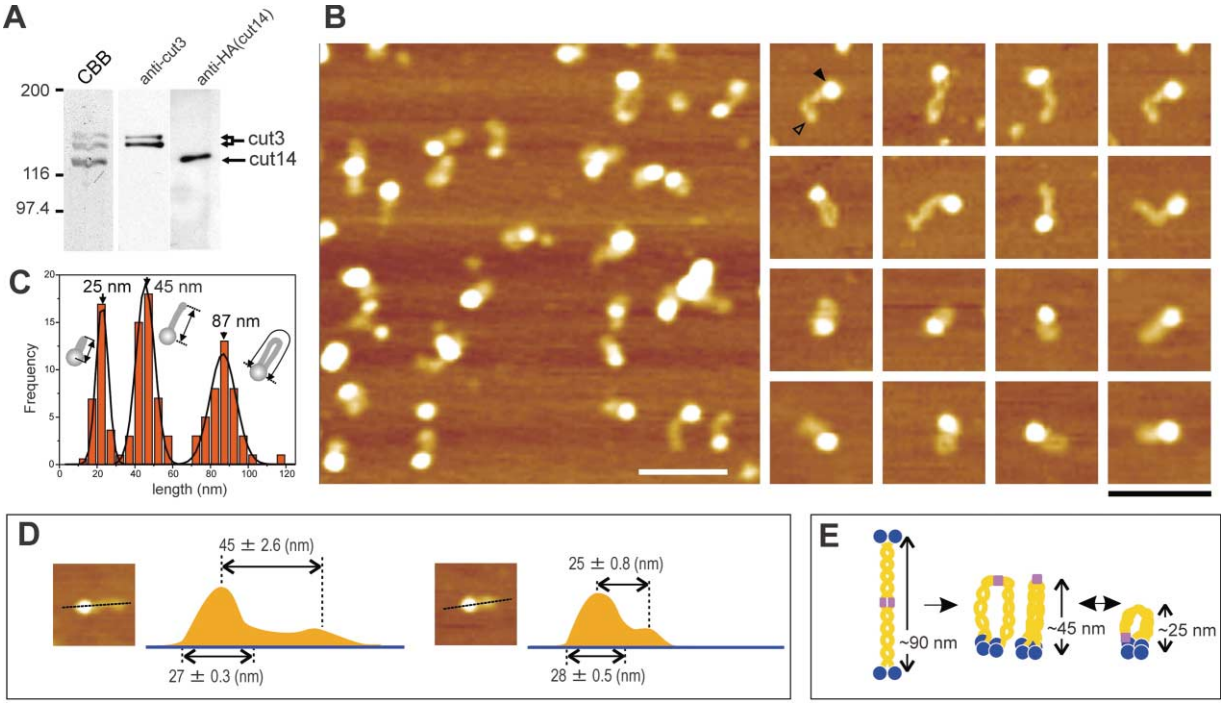

Figure 1. Purification and AFM Observation of the Fission Yeast Condensin SMC Heterodimer

(A) SDS-PAGE analysis of the heterodimer (Cut3-Cut14) purified by the Ni-affinity column and gel filtration (see Experimental Procedures). Protein bands were stained by Coomassie brilliant blue (CBB) or detected with antibodies against Cut3 or HA. Lower molecular weight form of Cut3 was the product of a cleavage of ~100 amino acids at the N terminus. The positions of protein standards (200, 116, 97.4 kDa) are shown.

(B) Two types of the head-tail particles with different tail lengths (longer tail, upper two rows in the right panels; shorter tail, lower two rows) were seen. The head (filled triangle) consists of four globular domains, and the tip of the tail (open triangle) represents the hinge region. Scale bars, 100 nm.

(C) Histograms of measured tail lengths. When the tail appeared duplicated, the entire length was measured and averaged (87 nm). The average length of singular-looking tails was 45 ± 2.6 nm and 25 ± 0.8 nm.

(D) Cross-section views of AFM images of 45 and 25 nm tails.

(E) A hypothetical heterodimer structure. In the long-tail structure, coiled-coil regions (yellow) were folded back at the hinge (red), and four globular domains (blue) are assembled. In short-tail structure, hinge is also assembled with globular domains.

during the preparation, the cohesin holocomplex [13] has not been observed.

Expression, Purification, and Observation of Condensin Trimer and Pentamer Complex

To purify the trimeric non-SMC complex of condensin, if it is formed, we constructed a *S. pombe* strain which overproduced simultaneously three subunits: Cnd1, Cnd2, and Cnd3. The amino terminus of the Cnd2 was tagged with 6H, and the tagged protein was shown to be functional (data not shown). The Ni column followed by Superose gel filtration allowed us to isolate the trimeric complex. AFM showed that the trimeric complex formed spherical particles (see Supplementary Material). Statistical analysis of the diameters produced two peaks in a histogram. A similar calculation suggests that the diameter of the 36 nm particle corresponds to a molecular mass of 350 kDa, which fits to the trimer. The 31 nm particle might have lost Cnd2. Three non-SMC subunits can polymerize into a trimer without the SMC heterodimer.

The heteropentamer was also purified using the tagged Cnd2 for affinity purification. Cnd2-HAH6 was simultaneously overexpressed with the four other subunits, Cut3, Cut14, Cnd1, and Cnd3, in *S. pombe* cells by the inducible promoter *nmt1*. The isolated condensin subunits were coeluted in gel filtration. SDS-PAGE analysis and immunoblotting revealed five subunits with the expected MWs (Figure 2A). Cut14 and Cnd1 migrate together as a single thick band when it is stained by CBB. Thus, the purified heteropentamer complex contains almost equal ratios of the five subunits. The fraction with the highest purity (fraction 22) was used for AFM.

The condensin complex showed basically two types of images, as shown in Figure 2B. The common type had a large head with a 45 nm or a 25 nm tail giving a "tadpole" like appearance (Figures 2C and 2D). The head (the average diameter, 36 ± 0.6 nm) is significantly larger than that of SMC heterodimer and has almost an identical size to that of the non-SMC trimer, indicating that the non-SMC trimer binds to the head of SMC heterodimer to form a heteropentamer. A "paired" structure with two heads and two tails was also found infrequently (less than 1%; examples shown in Figure 2B, bottom row). A model for these images is depicted in Figure 2E. The non-SMC trimer associates with the head or a coiled-coil region near the head [18]. Similar to the SMC

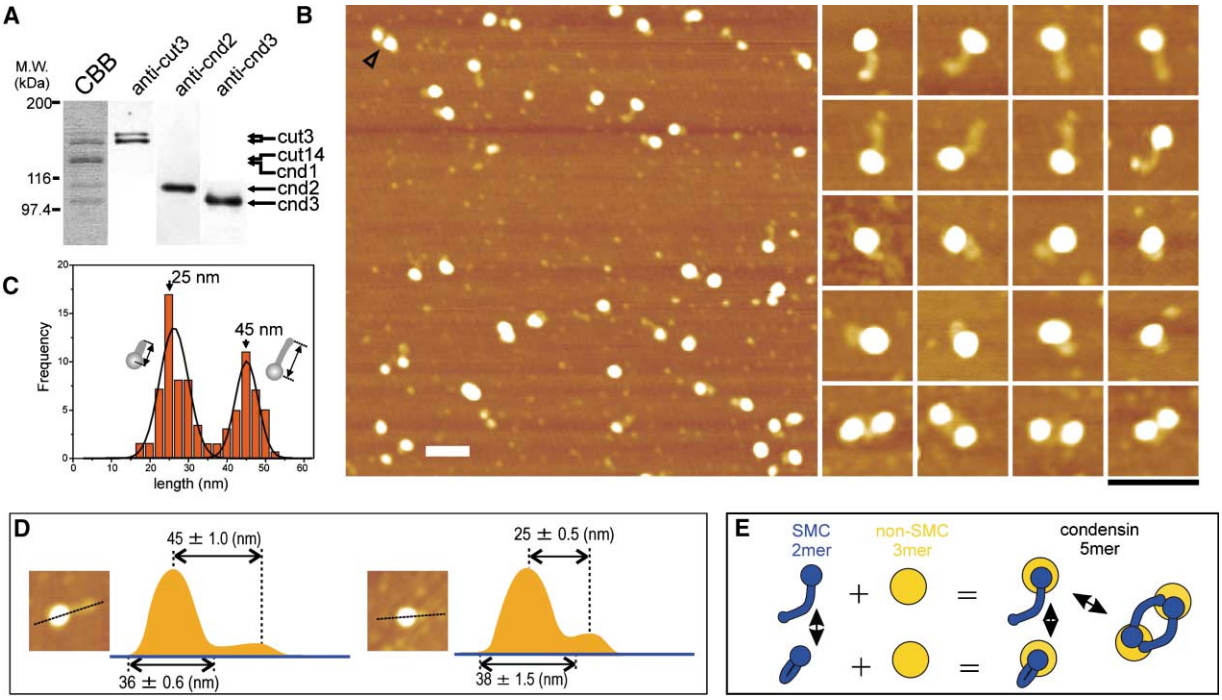

Figure 2. Purification and AFM Observation of the Condensin Heteropentamer Complex

(A) SDS-PAGE of the purified heteropentamer containing Cut3, Cut14, Cnd1, Cnd2, and Cnd3. Positions of the protein bands identified by immunoblotting are also indicated.

(B) AFM images of condensin heteropentamer complex. In the gallery, tadpole-like particles with longer tail (upper two rows) and shorter tail (middle two rows) are shown. Paired particles (open triangle, see text) are shown at the bottom row. Scale bars, 100 nm.

(C) Histograms for the lengths of the tails. Two types of the particles with short (25 nm) or long (45 nm) tail were observed.

(D) Cross-section views of the complex with two different tail lengths.

(E) A scheme for the stepwise formation of heteropentamer from SMC heterodimer and non-SMC heterotrimer. Open figures commonly seen for bacterial SMC were not observed under our experimental conditions.

heterodimer, the tip of the 45 nm tail associates with the head to form a short tail particle.

SMC Heterodimer-Dependent DNA Aggregation

To study the interaction in vitro between condensin and DNA, we first performed AFM observation of the heterodimer bound to ~1 μm long (~3.3 kb) duplex DNA derived from the innermost centromere region of *S. pombe* chromosome I. Characteristically, a large assembly of heterodimers was observed in association with DNA (Figure 3A). Such an aggregate formation among heterodimers was not seen in the absence of DNA, indicating that the assembly appears to be DNA dependent. Similar protein aggregates were made with noncentromeric DNA so that the sequence specificity is not high (data not shown). Importantly, the path of DNA free from protein association was much shorter than 1 μm (346 ± 15 nm), indicating that DNA within the aggregate was folded (Figure 3B). Taken together, the mode of association between heterodimers and DNA and between heterodimers seemed to be cooperative or the all-or-none type. Many DNA molecules were either free from protein or bound into a large assembly. This might be due to enhanced protein-protein interaction between heterodimers upon interaction with DNA [6, 19]. Alternatively, a conformational change of DNA, which facilitated association of heterodimers, might take place.

The gel-shift assay was done for the purified condensin SMC heterodimer as well as the heteropentamer (Figure 3C). The ^{32}P-labeled double-strand DNA was mixed and incubated with different concentrations of SMC heterodimer (left) and heteropentamer (right) and was run in native 8% acrylamide gel electrophoresis. Autoradiography shows the highly shifted band close to the well for the SMC heterodimer (open arrow). Higher concentrations of the SMC heterodimer increased the intensity of the band and produced no intermediate band. These results are consistent with the AFM observation that large protein aggregates were seen in a subpopulation of 3.3 kb long double-strand DNA molecules (Figure 3B). In sharp contrast, the heteropentamer complex produced no band close to the well but faint intermediate bands (filled arrows), suggesting that DNA is bound to one or two complexes in a distributive fashion.

AFM observation shows that the heteropentamer complex was dispersed in association with DNA (Figure 4A). Protein aggregates were not seen, and the individual tadpole-like particles bound to DNA could be observed. This is consistent with the gel-shift assay of the heteropentamer (Figure 3C). The tip of the tail seemed to be bound to DNA, indicating that the hinge and/or nearby coiled-coil region are the sites for scattered association of the heteropentamer with DNA. We presumed that non-SMC trimers played a negative regula-

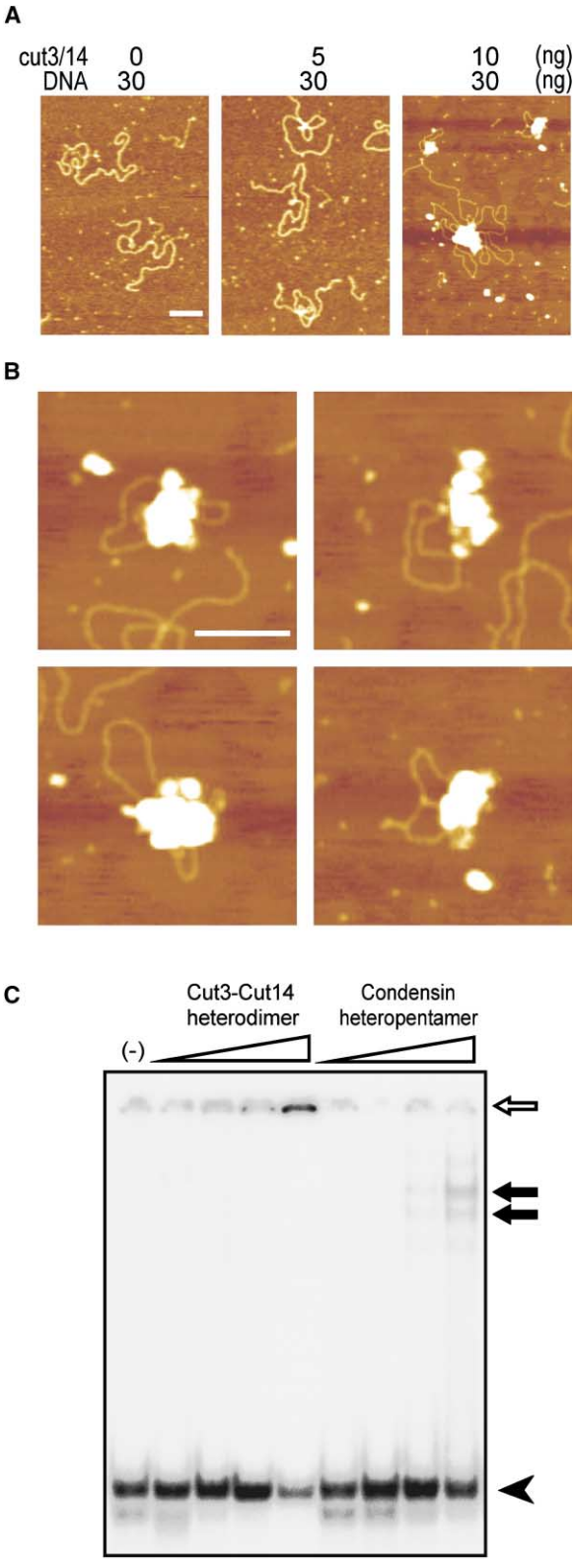

Figure 3. AFM Observation of the Heterodimer Bound to Duplex DNA

(A) Cut3-Cut14-dependent DNA aggregation. Purified Cut3-Cut14 heterodimers (0, 5, or 10 ng) were incubated with a constant concentration of ~3.3 kb (~1 μm long) linear duplex DNA (30 ng). Large protein aggregates were observed with 10 ng of heterodimers. Scale bar, 100 nm.

(B) High-magnification images of protein-DNA complexes. The path of DNA free from proteins was 345 ± 15 nm, much shorter than 1 μm. Scale bar, 100 nm.

(C) Gel shift assay of DNA binding by the condensin SMC heterodimer (left) and the heteropentamer (right). Autoradiography is shown with an arrowhead for the position of DNA bands without interaction. Arrows indicate the bands shifted after association. The SMC heterodimer produced the shifted band close to the well (open arrow), whereas discrete faint bands were seen for the heteropentamer (filled arrows).

tory role for the SMC heterodimer to form a large assembly on DNA.

ATPase Activity of Condensin Complex

We then measured the ATPase activity of the heteropentamer complex purified by a Ni column followed by gel filtration, in the absence (hatched columns, Figure 4B) or the presence (open columns) of DNA (mixture of linear and circular duplex DNA). The condensin SMC heterodimer itself did not produce any ATPase activity [8]. The fraction 22 showing the highest ATPase activity contained the most purified heteropentamer, but the fraction 25 also assayed contained the activity. Immunodepletion of the fraction 22 by anti-HA immunobeads abolished the ATPase activity. The addition of DNA stimulated the ATPase activity by 2- to 4-fold. These results indicated that, although the heteropentamer was obtained from growing cells largely consisting of interphase cells, it did have the DNA-stimulated ATPase activity as frog M phase condensin does[20], though the specific activity was roughly one-fifth of the frog M phase condensin. AFM did not produce any recognizable structural differences in the heteropentamer in the absence or the presence of ATP (data not shown). The overproduction system for mitotic heteropentamer has not been successful.

This is the first analysis of condensin architecture and the interaction with DNA by the combined methods of AFM and biochemical and genetical analysis. AFM observation of condensin SMC heterodimer and heteropentamer established that the non-SMC heterotrimer subunits were bound to the globular domains of the heterodimer. Thus, the ATPase domains of the heterodimer could be structurally regulated by the non-SMC trimer. The head opening that is observed in bacterial SMC might be regulated by the non-SMC subunits in eukaryotic condensin and cohesin. In the heteropentamer, the non-SMC trimer restrains the accessibility of head domain to the DNA, which results in dispersed binding along the DNA via the hinge region (Figure 4A). Our results are consistent with association of the head of SMC-like Rad50 with Mre11 nuclease [18] and requirement of non-SMC subunits for the condensin ATPase activation [21]. It is tempting to speculate that the opening of the SMC heterodimer head occurs for chromosome condensation in mitosis and is regulated by a transient gate opening by the non-SMC trimer in the presence of ATP in order to enclose the duplex DNAs for forming a loop (Figure 4C). Mitotic condensation is possibly caused by the formation of many DNA loops. For the case of cohesin, the cleavage of a non-SMC protein Scc1/Rad21 might allow transient

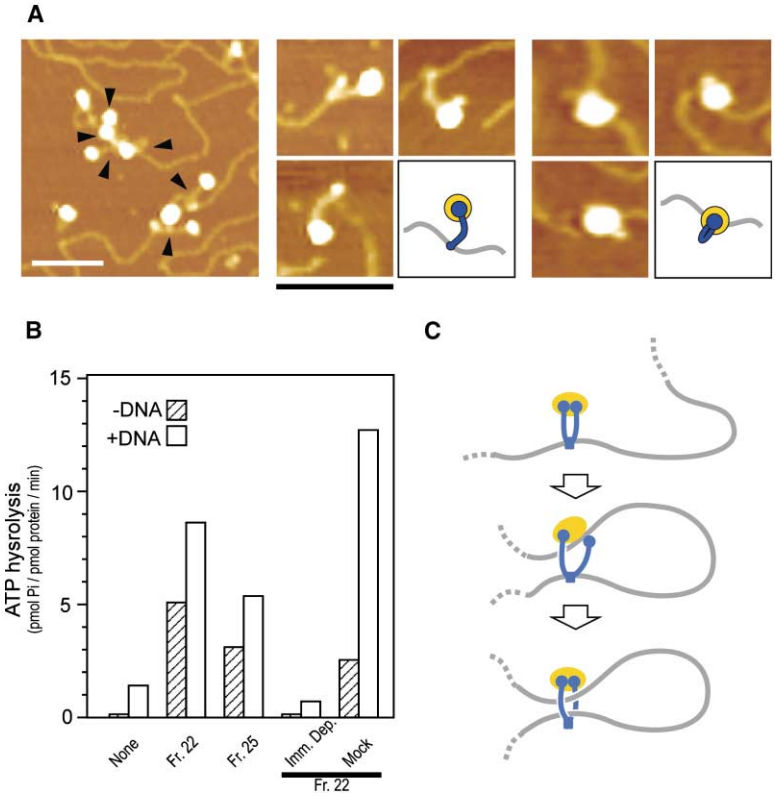

Figure 4. AFM Images and DNA-Stimulated ATPase Activity of the Heteropentamer

(A) AFM images of the condensin heteropentamer bound to duplex DNA. (Left panel) Low-magnification image of the heteropentamer complex incubated with the ~3.3 kb duplex DNA. Single individual particles are scattered along DNA (indicated by triangles). (Right panels) High-magnification images showing that the tip of the tail appears to be associated with DNA. Cartoons illustrating the mode of association are also shown. Scale bars, 100 nm.

(B) ATPase activity of the heteropentamer was measured in the presence (open columns) or the absence (hatched columns) of DNA as described in the text. Fraction 22 contained the highest concentration of the condensin and was either immunodepleted (treated with antibody-bound beads) or mock depleted (only beads).

(C) A hypothetical illustration of condensin complex associating with DNA. The hinge of condensin first interacts with DNA. Chromosome DNA may be then condensed by loop formation through gate opening of the non-SMC subunits followed by the enclosure of two duplex DNAs within the SMC subunits.

opening of SMC heterodimer for releasing the separated chromatid DNAs. AFM employed in this study was based on the conventional air-drying procedure and could be improved with better resolution by newly developing liquid methods [22, 23]. Further biochemical and ultrastructural study may elucidate cooperative protein-DNA assembly induced by aggregation of condensin SMC heterodimers, which might mimic chromosome condensation. Such an assumption is not contradictory to the activity of ATP-dependent, positive DNA supercoiling of frog 13S condensin, because the supercoiling is not catalytic and requires a stoichiometric amount of condensin [20, 24]. DNA-dependent aggregation of condensin SMC heterodimer resembles intermolecular interaction of bacterial SMC, which seems to activate ATPase [6]. Further work definitely requires the use of the heteropentamer from the M phase cells to understand how the complex is mechanistically activated from the interphase state.

Experimental Procedures

Plasmid Constructions

Simultaneous overproduction and purification of SMC subunits of condensin were performed as described previously [8]. The non-SMC genes *cnd1*$^+$, *cnd2*$^+$, and *cnd3*$^+$ were fused to the *nmt1* promoter and tandemly inserted into pUC119 with the *ura4*$^+$ marker and the *ars1*. The *cnd2*$^+$ gene was N-terminally tagged with six-histidine sequence for affinity purification (plasmid pET129). For the production of heteropentamer complex in yeast, the *cut3*$^+$ and *cut14*$^+$ genes, each of which is fused to the *nmt1* promoter, were tandemly inserted into the pUC119 vector with the *LEU2* marker gene and the *ars1* sequence (plasmid pET115). The non-SMC genes *cnd1*$^+$, *cnd2*$^+$, and *cnd3*$^+$ were also fused to the *nmt1* promoter and similarly cloned into pUC119 with the *ura4*$^+$ marker and the *ars1* (plasmid pET110). The *cnd2*$^+$ gene was C-terminally tagged with HA and six-histidine sequences for affinity purification.

Protein Purification

The fission yeast expressing the condensin subunits was cultured in minimal EMM2 medium in the absence of thiamine for 30 hr at 26°C. Subsequent purification steps were done at 0°C–4°C. Cells (~2 × 10^{10}) were washed once in lysis buffer (40 mM Tris at pH 7.5, 60 mM β-glycerophosphate, 50 mM NaCl, 2 mM $MgCl_2$, 10% Glycerol, 0.1% NP-40) and disrupted by glass beads in 12 ml of lysis buffer containing protease inhibitors (1 mM PMSF and protease inhibitor cocktail; Sigma). The cell lysates were centrifuged at 40,000 rpm for 1 hr using a Beckman 60Ti rotor, and the supernatant was bound to 1 ml of Ni-NTA agarose (Qiagen) for 2 hr. The resin was washed twice with 10 ml of the lysis buffer containing 20 mM imidazole, and the bound proteins were eluted with 5 ml of the lysis buffer containing 200 mM imidazole. A fraction containing condensin subunits was concentrated with Microcon 50 (Amicon) and injected to Superose 6 (HR 10/30; Amersham Pharmacia) equilibrated with the buffer S (20 mM Tris-Cl [pH 7.5], containing 200 mM NaCl, 10% Glycerol, 0.02% NP-40, 1 mM 2-mercaptoethanol, and 0.1 mM PMSF).

Gel Retardation Assay

Two complementary oligonucleotides (5′-32P-CCCTATAACCCCT GCATTGAATTCCAGTCTGATAA-3′ and 5′-TTATCAGACTGGAATT CAATGCAGGGGTTATAGGG-3′) were annealed in 10 mM Tris at pH 7.5 containing 50 mM NaCl, 10 mM $MgCl_2$, and 1 mM dithiothreitol (DTT), and purified by polyacrylamide gel electrophoresis. The end-labeled double-stranded DNA was incubated with condensin protein complex purified by gel filtration in total 20 μl of the binding buffer (20 mM Tris at pH 7.5, 50 mM NaCl, 2 mM $MgCl_2$, 10% glycerol, 1 mM DTT, 0.1 mg/ml BSA) at the room temperature for 1 hr. The sample was run in 8% nondenaturing polyacrylamide gel, followed by autoradiography.

ATPase Assay

The ATPase assay was performed based on the reference [20].

AFM Imaging

Purified condensin complex was diluted with 5 mM HEPES (pH 7.4) and incubated on ice for 30 min with or without the indicated amount of DNA (3.3 kb PCR fragment containing a centromere region of *S. pombe* chromosome I). Fixation with 0.25%–0.5% glutaraldehyde for 1–7 hr on ice was done when necessary. For the AFM imaging, 0.5–1 ng of condensin complex was applied on the freshly cleaved mica surface, which is pretreated with 10 mM spermidine. After 10 min, the mica was gently washed with water and dried with nitrogen gas. The AFM imaging was performed with Nanoscope IIIa (Digital Instrument, CA) with a type E scanner under the Tapping Mode™ in air at room temperature. The AFM probes made of single silicon crystal with a cantilever length of 129 μm and a spring constant 33–62 N/m (OLYMPUS) were used. Images were collected in height mode and stored in the 512 $\times$ 512 pixel format. The images obtained were then plane fitted and analyzed by the computer program accompanied with the imaging module.

Supplementary Material

Supplementary Material including figures showing purification and AFM observation of SMC heterodimer of cohesin and purification and AFM observation of the non-SMC heterotrimer complex can be found online at http://images.cellpress.com/supmat/supmatin.htm.

Acknowledgments

This study was supported by the CREST research project of the Japan Science and Technology Corporation (to M.Y. and to K.T), the Special Co-ordination Funds (to K.T), and the COE Research Grant from the Ministry of Education, Culture, Sports, Science and Technology of Japan. S.H.Y and T.S. are recipients of the Japan Society for the Promotion of Science pre- and postdoctoral fellowships, respectively.

Received: January 2, 2002
Revised: January 30, 2002
Accepted: January 30, 2002
Published: March 19, 2002

References

1. Hirano, T. (1999). SMC-mediated chromosome mechanics: a conserved scheme from bacteria to vertebrates? Genes Dev. *13*, 11–19.
2. Jessberger, R., Frei, C., and Gasser, S.M. (1998). Chromosome dynamics: the SMC protein family. Curr. Opin. Genet. Dev. *8*, 254–259.
3. Strunikov, A.V. (1998). SMC proteins and chromosome structure. Trends Cell Biol. *8*, 454–459.
4. Hopfner, K.P., Karcher, A., Shin, D.S., Craig, L., Arthur, L.M., Carney, J.P., and Tainer, J.A. (2000). Structural biology of Rad50 ATPase: ATP-driven conformational control in DNA double-strand break repair and the ABC-ATPase superfamily. Cell *101*, 789–800.
5. Melby, T.E., Ciampaglio, C.N., Briscoe, G., and Erickson, H.P. (1998). The symmetrical structure of structural maintenance of chromosomes (SMC) and MukB proteins: long, antiparallel coiled coils, folded at a flexible hinge. J. Cell Biol. *142*, 1595–1604.
6. Hirano, M., Anderson, D.E., Erickson, H.P., and Hirano, T. (2001). Bimodal activation of SMC ATPase by intra- and inter-molecular interactions. EMBO J. *20*, 3238–3250.
7. Saka, Y., Sutani, T., Yamashita, Y., Saitoh, S., Takeuchi, M., Nakaseko, Y., and Yanagida, M. (1994). Fission yeast cut3 and cut14, members of the ubiquitous protein family, are required for chromosome condensation and segregation in mitosis. EMBO J. *13*, 4938–4952.
8. Sutani, T., and Yanagida, M. (1997). DNA renaturation activity of the SMC complex implicated in chromosome condensation. Nature *388*, 798–801.
9. Hirano, T. (2000). Chromosome cohesion, condensation, and separation. Annu. Rev. Biochem. *69*, 115–144.
10. Koshland, D., and Strunnikov, A. (1996). Mitotic chromosome condensation. Annu. Rev. Cell Dev. Biol. *12*, 305–333.
11. Nasmyth, K. (1999). Separating sister chromatids. Trends Biochem. Sci. *24*, 98–104.
12. Losada, A., Hirano, M., and Hirano, T. (1998). Identification of *Xenopus* SMC protein complexes required for sister chromatid cohesion. Genes Dev. *12*, 1986–1997.
13. Tomonaga, T., Nagao, K., Kawasaki, Y., Furuya, K., Murakami, A., Morishita, J., Yuasa, T., Sutani, T., Kearsey, S.E., Uhlmann, F., et al. (2000). Characterization of fission yeast cohesin: essential anaphase proteolysis of Rad21 phosphorylated in the S phase. Genes Dev. *14*, 2757–2770.
14. Hirano, T., Kobayashi, R., and Hirano, M. (1997). Condensins, chromosome condensation protein complexes containing XCAP-C, XCAP-E and a *Xenopus* homologue of the *Drosophila* Barren protein. Cell *89*, 511–521.
15. Sutani, T., Yuasa, T., Tomonaga, T., Dohmae, N., Takio, K., and Yanagida, M. (1999). Fission yeast condensin complex: essential roles of non-SMC subunits for condensation and Cdc2 phosphorylation of Cut3/SMC4. Genes Dev. *13*, 2271–2283.
16. Freeman, L., Aragon-Alcaide, L., and Strunnikov, A. (2000). The condensin complex governs chromosome condensation and mitotic transmission of rDNA. J. Cell Biol. *149*, 811–824.
17. Bustamante, C., Keller, D., and Yang, C. (1993). Scanning force microscopy of nucleic acids and nucleoprotein assemblies. Curr. Opin. Struct. Biol. *3*, 363–372.
18. Hopfner, K.P., Karcher, A., Craig, L., Woo, T.T., Carney, J.P., and Tainer, J.A. (2001). Structural biochemistry and interaction architecture of the DNA double-strand break repair Mre11 nuclease and Rad50-ATPase. Cell *105*, 473–485.
19. Hirano, M., and Hirano, T. (1998). ATP-dependent aggregation of single-stranded DNA by a bacterial SMC homodimer. EMBO J. *17*, 7139–7148.
20. Kimura, K., and Hirano, T. (1997). ATP-dependent positive supercoiling of DNA by 13S condensin: a biochemical implication for chromosome condensation. Cell *90*, 625–634.
21. Kimura, K., and Hirano, T. (2000). Dual roles of the 11S regulatory subcomplex in condensin functions. Proc. Natl. Acad. Sci. USA *97*, 11972–11977.
22. Bustamante, C., Smith, S.B., Liphardt, J., and Smith, D. (2000). Single-molecule studies of DNA mechanics. Curr. Opin. Struct. Biol. *10*, 279–285.
23. Engel, A., Gaub, H.E., and Muller, D.J. (1999). Atomic force microscopy: a forceful way with single molecules. Curr. Biol. *9*, R133–136.
24. Kimura, K., Rybenkov, V.V., Crisona, N.J., Hirano, T., and Cozzarelli, N.R. (1999). 13S condensin actively reconfigures DNA by introducing global positive writhe: implications for chromosome condensation. Cell *98*, 239–248.